Journal of New Results in Science
https://dergipark.org.tr/en/pub/jnrs
Research Article
Open Access

E-ISSN:1304-7981 https://doi.org/10.54187/jnrs.851917

Magnetohydrodynamic peristaltic transport of Casson fluid embedded with chemical reaction in an asymmetrical permeable conduit

Asha Kotnurkar[1], Chandrashekhar Hadapad[2]

Keywords:
Magnetohydrodynamic,
Peristaltic transport,
Casson fluid,
Chemical reaction,
Porous medium.

Abstract — The present study investigates the magnetohydrodynamic non-Newtonian peristaltic flow of the Casson fluid model embedded with a chemical reaction. The assumption of small Reynolds number and approximations of long-wavelength are considered. The constituent equations are analytically solved by the method of decomposition by Adomian. Distributions of the velocity field, pressure gradient and concentration field are obtained. The simulations of influencing parameters on the behaviour of the fluid model have been elaborated with the help of graphs, and detailed analysis has been done. It can be observed that both the reaction parameter and Schmidt Number show similar behaviour for concentration profile. The graphs clearly show that the fluid parameter drastically reduces the pressure rise and pressure gradient. The pressure gradient will be increased by the increase in Hartmann number, but it reduces the pressure rise.

Subject Classification (2020):

1. Introduction

Peristalsis refers to a spontaneous wave mechanism like muscular contractions of the digestive tract or other tube-like structures. It is characterised by alternating contraction and relaxation, which helps push indigested food through the digestive duct towards its release at the anus. The pioneering work in this regard was initiated by starling and Bayliss [1], who described it as an ability of fluid to move or get around. Some of the peristaltically governing bodily flows are organs of the digestive system, oesophagus and intestine. Latham [2] study on peristaltic transport is influenced many researchers to develop many experimental and theoretical studies to understand the mechanical behaviour of fluids in different conditions. These works have been done by incorporating blood and other bodily fluids as Newtonian fluids. But it is much more significant to study the peristaltic transport of Bio-fluids by considering them as non-Newtonian fluids as human blood in arterioles, intestine etc., behave like a non-Newtonian fluid.

A key point in considering the non-Newtonian fluid model ahead of the Newtonian model is its viscosity, which is dependent on the forces being applied to it. Some of the applications include syrup drugs, toothpaste, colloids. A Casson fluid model with a distinct feature and its rheological behaviour

[1]as.kotnur2008@gmail.com (Corresponding Author); [2]chandruh.h4@gmail.com
[1]Department of Mathematics, Karnatak University, Dharwad, India.
[2]Department of Mathematics, Karnatak University, Dharwad, India.
Article History: Received: 01 Jan 2021 — Accepted: 31 Dec 2021 — Published: 31 Dec 2021

was pioneered by Casson [3]. Some more research work related to the peristaltic transport of the Casson model is seen in refs. [4-10].

However, studies related to a complex interaction of peristaltic motion of conducting fluid with extremely imposed magnetic field will enhance a better understanding of the performance of conductive physiological fluids like blood flow in small vessels (Casson fluid model), blood pump machines etc., Magnetohydrodynamics (MHD) or Magento fluid dynamics deal with magnetic properties and nature of fluids which easily have electrons pass through them, for instance, blood plasmas, saline. The motive behind using MHD is that applied magnetic fields can trigger currents in a flowing conductive fluid, which polarizes the fluid and that inertly changes the magnetic field itself. Some applications include sensors, casting by electromagnetic radiation, power generation with MHD, drug targeting by the applied magnetic field. Magneto hydrodynamic equations analyse the correlation between the external magnetic field and magnetic fluid particles in the bloodstream [11-23].

In many industrial and technological fields, problems that deal with differences in temperature and concentration difference have importance on chemical reaction processes. This phenomenon has its role in the conduction of heat and mass in a fluid motion. Chemical reactions are essential to chemical engineering, fluid dynamics, where they can be utilised to produce new compounds from naturally occurring raw materials like ores and petroleum. Related work can be seen in [24-32].

A semi-analytical method has been adopted to solve subsequent governing non-linear partial differential equations. This method allows a non-linear portion of the differential equation for solution convergence. Motivated by this, we attempted to analyse Casson fluid's peristaltic transport by the Adomian Decomposition Method (ADM). MHD and chemical reaction effects are considered. We have discussed the present study results through graphs, and the impact of pertinent parameters like rate of chemical reaction, Hartmann number and fluid parameter on pressure gradient, flow rate and, concentration profile are analysed in detail.

2. Problem formulation

The peristaltic motion of a steady condensed MHD Casson fluid model is considered with chemical reaction in a 2D channel with asymmetry at the walls. Where $\left(\overline{X}', \overline{Y}'\right)$ is the coordinate with $\overline{X}'$ along the direction of wave and $\overline{Y}'$ perpendicular to $\overline{X}'$ axis. The motion of the fluid model is driven by the sine wave having a constant speed c along the channel walls. The description of the walls is given by $\bar{Y} = \overline{h_1}'$ and $\bar{Y} = \overline{h_2}'$ representing the boundaries of the channel (Figure 1).

$$\overline{h_1}'(\overline{X}', \bar{t}) = d_1 + a_1 \operatorname{Cos}[\frac{2\pi}{\lambda}(\overline{X}' - c\bar{t})], \text{ upper wall} \tag{2.1}$$

$$\overline{h_2}'(\overline{X}', \bar{t}) = d_2 - a_2 \operatorname{Cos}[\frac{2\pi}{\lambda}(\bar{\varphi} + \overline{X}' - c\bar{t})]. \text{ lower wall} \tag{2.2}$$

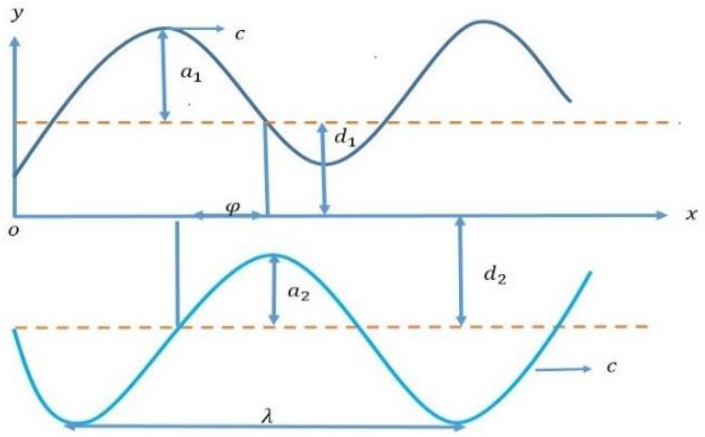

Figure1. A physical model of asymmetric channel.

where a_2, a_1 the amplitude of the lower wall waves is λ the wavelength, time $\bar{t}$, phase- difference φ. It is noted that for the symmetric channel, $\varphi = 0$ that means waves out of phase and $\varphi = \pi$ waves are in phase. and d_2, d_1 satisfies a criterion: $a_1^2 + 2b_1 a_1 \cos\varphi + b_1^2 \le d_2^2 + d_1^2$.

Vector form of velocity V is $V = (\overline{U}, \overline{V}, 0)$ where $\overline{U}, \overline{V}$ are the velocity coordinates of the velocity field in the laboratory frame of reference.

The Rheological model of a Casson fluid is

$$\tau_{ij} = (\mu_0 + \frac{\rho_y}{\sqrt{2\pi_c}})2e_{ij}, \quad \text{when } \pi < \pi_c \tag{2.3}$$

$$\tau_{ij} = (\mu_0 + \frac{\rho_y}{\sqrt{2\pi_c}})2e_{ij}, \quad \text{when } \pi > \pi_c \tag{2.4}$$

Where ρ_y is the fluid yield stress, expressed as:

$$\rho_y = \frac{\mu_0\sqrt{2\pi}}{\beta}, \tag{2.5}$$

μ_0 is the fluid's plastic dynamic viscosity.

π is given by $\pi = e_{ij}.e_{ij}$.

e_{ij} - $(i, j)^{th}$ is the constituent of deformation rate and

π_c is the critical value relying on the non-Newtonian behaviour.

Denoting the velocity components $\overline{U}$ and $\overline{V}$ respectively along with X, Y directions in a fixed frame.

The governing equations of the flow are defined as:

$$\rho\left(\overline{U}\frac{\partial\overline{U}}{\partial\overline{X}}+\overline{V}\frac{\partial\overline{U}}{\partial\overline{Y}}+\frac{\partial\overline{U}}{\partial\overline{t}}\right)=\mu_B\left(1+\frac{1}{\gamma}\right)\left(\frac{\partial^2\overline{U}}{\partial x^2}+\frac{\partial^2\overline{U}}{\partial y^2}\right)-\sigma\overline{B_0}^2\overline{U}-\frac{\mu_B\overline{U}}{K_1}+\rho g\beta(\overline{C}-\overline{C_0})-\frac{\partial\overline{P}}{\partial\overline{X}}, \tag{2.6}$$

$$\rho\left(\frac{\partial\overline{V}}{\partial\overline{t}}+\overline{U}\frac{\partial\overline{V}}{\partial\overline{X}}+\overline{V}\frac{\partial\overline{V}}{\partial\overline{Y}}\right)=-\frac{\partial\overline{P}}{\partial\overline{Y}}+\mu_B\left(1+\frac{1}{\gamma}\right)\left(\frac{\partial^2\overline{V}}{\partial x^2}+\frac{\partial^2\overline{V}}{\partial y^2}\right)-\sigma\overline{B_0}^2\overline{V}-\frac{\mu_B\overline{V}}{K_1}, \tag{2.7}$$

$$\left(\overline{U}\frac{\partial\overline{C}}{\partial\overline{X}}+\overline{V}\frac{\partial\overline{C}}{\partial\overline{Y}}+\frac{\partial\overline{C}}{\partial\overline{t}}\right)=D_B\left(\frac{\partial^2\overline{C}}{\partial\overline{Y}^2}+\frac{\partial^2\overline{C}}{\partial\overline{X}^2}\right)-k_1(\overline{C}-\overline{C_0}), \tag{2.8}$$

where $\overline{V}$ and $\overline{U}$ are the velocity components along with the Y, X directions, respectively, ρ denotes the fluid's density, μ_B - viscosity of the fluid, γ the Casson parameter, $\overline{P}$ - pressure, σ - fluid's electrical conductivity, B_0 the applied magnetic field, β volumetric expansion coefficient, C the concentration, D_B the Brownian diffusion coefficient, g is the acceleration due to gravity, K_1 the thermal conductivity of the fluid as seen in Equations 2.6-2.8 respectively.

The flow can be considered unsteady if seen in the laboratory frame; however, in a coordinate plane moving at speed c in the wave frame (x, y), it can be treated as steady.

In two frames, velocities, coordinates, pressure, and concentration are

$$x=\overline{X}+(-c)\overline{t},\ u=\overline{U}+(-c),\ y=\overline{Y},\ v=\overline{V},\ c=\overline{C},\ p=\overline{P},$$

Here $\overline{U},\overline{V}$ and u,v are the components of velocity for the corresponding Cartesian systems.

The dimensional boundary conditions are

$$\overline{U}=-c\ ,\quad \overline{C}=\overline{C_0}\qquad \text{at}\quad y=\overline{h_1}', \tag{2.9}$$

$$\overline{U}=-c\ ,\quad \overline{C}=\overline{C_1}\qquad \text{at}\quad y=\overline{h_2}', \tag{2.10}$$

The following non-dimensional parameters are

$$\begin{gathered}u=\frac{\overline{U}}{c},\ v=\frac{\overline{V}}{c},\ t=\frac{c\overline{t}}{\lambda},\ p=\frac{\overline{P}d_1^2}{c\lambda\mu_B},\ x=\frac{\overline{X}}{\lambda},\ y=\frac{\overline{Y}}{d_1},\ Sc=\frac{\mu_B}{D},\ R'=\frac{k_1d_1^2}{\mu_B},\\ C=\frac{\overline{C}-\overline{C_0}}{\overline{C_1}-\overline{C_0}},\ \delta=\frac{d_1}{\lambda},\ M=\sqrt{\frac{\sigma}{\mu_B}}B_0d_1,\ Da=\frac{k}{d_1^2},\ G_m=\frac{\rho gB_cd_1^2(\overline{C_1}-\overline{C_0})}{c\mu_B}.\end{gathered} \tag{2.11}$$

In view of Equation 2.11, Equations 2.6 - 2.8, reduce to

$$\frac{\partial p}{\partial x}=\left(1+\frac{1}{\gamma}\right)\frac{\partial^2u}{\partial y^2}-\left(M^2+\frac{1}{k}\right)u+G_mC, \tag{2.12}$$

$$\frac{\partial^2C}{\partial y^2}=ScR'C, \tag{2.13}$$

The dimensionless boundary conditions are

$$C = 0, u = 1, \quad \text{at } y = h_1, \tag{2.14}$$

$$C = 1, u = -1 \text{ at } y = h_2. \tag{2.15}$$

3. Method of solution

Using Adomian decomposition method, Equation 2.12 can be written as

$$L_{yy}u - N^2 u = \left\{ \frac{\gamma \dfrac{dp}{dx}}{1+\gamma} - \frac{G_m \gamma C}{1+\gamma} \right\}, \tag{3.1}$$

Where $N^2 = \dfrac{\left(M^2 + 1/k\right)\gamma}{1+\gamma}$, $L_{yy} = \dfrac{d^2}{dy^2}$,

Since L_{yy} is a second order differential operator, L_{yy}^{-1} is an inverse integration operator of order 2 defined by

$$L_{yy}^{-1}(.) = \int_0^y \int_0^y (.)dydy. \tag{3.2}$$

Employing L_{yy}^{-1}, Equation 3.1 becomes

$$u = C_1 + C_2 y + L_{yy}^{-1}\left(\frac{\gamma \dfrac{dp}{dx}}{1+\gamma} - \frac{G_m \gamma C}{1+\gamma} \right) + L_{yy}^{-1}\left(N^2 u\right). \tag{3.3}$$

By the semi-analytical Adomian Decomposition method we get

$$u = \sum_{n=0}^{\infty} u_n. \tag{3.4}$$

Equation 3.3 gives,

$$u_0 = C_1 + C_2 y + \left(\left(\frac{\gamma \dfrac{dp}{dx}}{1+\gamma} \right) \right) \frac{y^2}{2!} - \left(\frac{G_m \gamma}{1+\gamma} \right) \frac{Sinhk(y - h_1)}{k^2 Sinhk(h_2 - h_1)},$$

$$u_{n+1} = N^2 L_{yy}^{-1}(u_n), \ n \geq 0. \tag{3.5}$$

Using boundary conditions in Equation 2.14 and 2.15 to Equations 3.3-3.5, we obtain

$$u_1 = C_1 \frac{(Ny)^2}{2!} + \frac{C_2}{N} \frac{(Ny)^3}{3!} + \left(\left(\frac{\gamma}{N^2(1+\gamma)} \right) \frac{dp}{dx} \right) \frac{(Ny)^4}{4!} - \left(\frac{G_m \gamma}{1+\gamma} \right) \frac{N^2 Sinhk(y - h_1)}{k^4 Sinhk(h_2 - h_1)},$$

$$u_2 = C_1\frac{(Ny)^4}{4!}+\frac{C_2}{N}\frac{(Ny)^5}{5!}+\left(\left(\frac{\gamma}{N^2(1+\gamma)}\right)\frac{dp}{dx}\right)\frac{(Ny)^6}{6!}-\left(\frac{G_m\gamma}{1+\gamma}\right)\frac{N^4 Sinhk(y-h_1)}{k^6 Sinhk(h_2-h_1)},$$

$$u_3 = C_1\frac{(Ny)^6}{6!}+\frac{C_2}{N}\frac{(Ny)^7}{7!}+\left(\left(\frac{\gamma}{N^2(1+\gamma)}\right)\frac{dp}{dx}\right)\frac{(Ny)^8}{8!}-\left(\frac{G_m\gamma}{1+\gamma}\right)\frac{N^6 Sinhk(y-h_1)}{k^8 Sinhk(h_2-h_1)},$$

$$u_n = C_1\frac{(Ny)^{2n}}{2n!}+\frac{C_2}{N}\frac{(Ny)^{2n+1}}{(2n+1)!}+\left(\left(\frac{\gamma}{N^2(1+\gamma)}\right)\frac{dp}{dx}\right)\frac{(Ny)^{2n}}{2n!}-\left(\frac{G_m\gamma}{1+\gamma}\right)\sum_{n=0}^{\infty}\frac{N^{2n}}{k^{2n+2}}\left(\frac{Sinhk(y-h_1)}{Sinhk(h_2-h_1)}\right),$$

$$u = C_1 CoshNy+\frac{C_2}{N}SinhNy+\left(\left(\frac{\gamma}{N^2(1+\gamma)}\right)\frac{dp}{dx}\right)(CoshNy-1)-\left(\frac{G_m\gamma}{1+\gamma}\right)\left(\frac{1}{k^2-N^2}\right)\frac{Sinhk(y-h_1)}{Sinhk(h_2-h_1)}. \tag{3.6}$$

where

$$C_1 = \frac{1}{CoshNh_1}-\frac{SinhNh_1}{CoshNh_1}\left\{\frac{2CoshNh_1}{SinhN(h_1-h_2)}-\frac{CoshNh_1-CoshNh_2}{SinhN(h_1-h_2)}+\left(\frac{\gamma}{N^2(1+\gamma)}\right)\frac{dp}{dx}\right\}$$
$$\left\{\left(\frac{CoshNh_2-CoshNh_1}{SinhN(h_1-h_2)}\right)-\frac{G_m\gamma CoshNh_1}{(1+\gamma)(k^2-N^2)SinhN(h_1-h_2)}\right\}$$
$$-\frac{\gamma\, dp/dx}{N^2(1+\gamma)}\left(\frac{CoshNh_1-1}{CoshNh_1}\right)$$

$$\frac{C_2}{N} = \frac{2CoshNh_1}{SinhN(h_1-h_2)}-\frac{(CoshNh_1-CoshNh_2)}{SinhN(h_1-h_2)}+\left(\frac{\gamma}{N^2(1+\gamma)}\right)\frac{dp}{dx}\left(\frac{CoshNh_2-CoshNh_1}{SinhN(h_1-h_2)}\right)$$
$$-\frac{G_m\gamma CoshNh_1}{(1+\gamma)(k^2-N^2)SinhN(h_1-h_2)}$$

$k=\sqrt{scR'}$.

The flow rate in the (x,y) is given as

$$q=\int_{h_1}^{h_2} u\,dy. \tag{3.7}$$

$$q = \frac{\left(SinhNh_2-SinhNh_1\right)}{N\,CoshNh_1}-\frac{Sinh2Nh_1\left(SinhNh_2-SinhNh_1\right)}{N\,CoshNh_1\,SinhN(h_1-h_2)}+$$
$$\frac{SinhNh_1\left(CoshNh_1-CoshNh_2\right)\left(SinhNh_2-SinhNh_1\right)}{N\,CoshNh_1\,SinhN(h_1-h_2)}-$$
$$\frac{\gamma\frac{dp}{dx}\left(\begin{matrix}\left(CoshNh_1-1\right)SinhN(h_1-h_2)+\\ \left(CoshNh_2-CoshNh_1\right)SinhNh_1\end{matrix}\right)\left(SinhNh_2-SinhNh_1\right)}{N^3(1+\gamma)CoshNh_1\,SinhN(h_1-h_2)}+\frac{2\left(CoshNh_2-CoshNh_1\right)CoshNh_1}{N\,SinhN(h_1-h_2)}$$

$$+\frac{\left(CoshNh_2-CoshNh_1\right)^2}{N\,SinhN(h_1-h_2)}+\frac{\gamma\frac{dp}{dx}}{N^3(1+\gamma)}\left(\frac{\left(CoshNh_2-CoshNh_1\right)^2}{SinhN(h_1-h_2)}+\left(\left(SinhNh_2-SinhNh_1\right)-N(h_2-h_1)\right)\right)$$

$$-\frac{G_m\gamma}{(k^2-N^2)(1+\gamma)}\left(\frac{2\left(CoshNh_2-CoshNh_1\right)CoshNh_1}{N\,SinhN(h_1-h_2)}+\frac{\left(Coshk(h_2-h_1)-1\right)}{k\,Sinhk(h_2-h_1)}\right)$$

From Equation 3.7,

$$\frac{dp}{dx}=\left(\begin{array}{l}\dfrac{N^3(1+\gamma)\,CoshNh_1\,SinhN(h_1-h_2)}{\gamma\left(SinhN(h_1-h_2)CoshNh_1\left(\left(SinhNh_2-SinhNh_1\right)-N(h_2-h_1)\right)\right)+}\\ CoshNh_1\left(CoshNh_2-CoshNh_1\right)^2-\left(SinhNh_2-SinhNh_1\right)\left(\begin{array}{l}\left(CoshNh_1-1\right)SinhN(h_1-h_2)+\\ SinhNh_1\left(CoshNh_2-CoshNh_1\right)\end{array}\right)\end{array}\right)$$

$$\left(\begin{array}{l}q-\dfrac{\left(SinhNh_2-SinhNh_1\right)}{N\,CoshNh_1}+\dfrac{Sinh2Nh_1\left(SinhNh_2-SinhNh_1\right)}{N\,CoshNh_1\,SinhN(h_1-h_2)}+\\ \dfrac{SinhNh_1\left(SinhNh_2-SinhNh_1\right)\left(CoshNh_2-CoshNh_1\right)}{N\,CoshNh_1\,SinhN(h_1-h_2)}-\dfrac{2\left(CoshNh_2-CoshNh_1\right)CoshNh_1}{N\,SinhN(h_1-h_2)}-\\ \dfrac{\left(CoshNh_2-CoshNh_1\right)^2}{N\,SinhN(h_1-h_2)}+\dfrac{G_m\,\gamma}{(1+\gamma)\left(k^2-N^2\right)}\left(\begin{array}{l}\dfrac{k\,Sinhk(h_2-h_1)CoshNh_1\left(CoshNh_2-CoshNh_1\right)}{+\left(Coshk(h_2-h_1)-1\right)N\,SinhN(h_1-h_2)}\\ N\,k\;SinhN(h_1-h_2)Sinhk(h_2-h_1)\end{array}\right)\end{array}\right)$$

The dimensionless equation of the pressure rise is given by

$$\Delta p=\int_0^1\frac{dp}{dx}dx. \tag{3.8}$$

The volumetric flow rate at a given instant of the fixed frame is provided by,

$$\overline{Q}(x,t)=\int_{h_1'}^{h_2'}U'\left(X',Y',t'\right)dy', \tag{3.9}$$

where h_2' and h_1' are mappings of X' and Y' respectively.

In wave frame the rate of flow is given by,

$$q = \int_{h_2'}^{h_1'} u'\left(x', y'\right) dy'. \tag{3.10}$$

Utilising the transformations into the Equations 3.9 and 3.10, the entity among Q and q can be written as

$$Q = c(h_2' - h_1') + q. \tag{3.11}$$

The mean time flow for a period T at a constant position X' is given by

$$\bar{Q} = \frac{1}{T}\int_0^T Q\, dt. \tag{3.12}$$

Using Equation 3.12 in Equation3.11 the flow rate $\bar{Q}$ is,

$$\bar{Q} = \frac{1}{T}\int_0^T qdt + c(h_1' - h_2') = q + cd_2 + cd_1. \tag{3.13}$$

The dimensionless form of Equation 3.13 is given by

$$\theta = F + d + 1, \tag{3.14}$$

where $\theta = Q' / d_1 c$ and $F = q / d_1 c,$ such that

$$F = \int_{h_2}^{h_1} u\, dy = u(h_1 - h_2). \tag{3.15}$$

Solving Equation 2.13, with the boundary conditions in Equation2.14 and 2.15, we can obtain

$$C = ACoshky + \frac{B}{k} Sinhky,$$

where

$$A = \frac{-Sinhkh_1}{Sinhk(h_2 - h_1)}$$

$$B = \frac{k\,Coshkh_1}{Sinhk(h_2 - h_1)}$$

$$k = \sqrt{ScR'}$$

This may be simplified as

$$C = \frac{Sinhk(y - h_1)}{Sinhk(h_2 - h_1)}. \tag{3.16}$$

The expression determining velocity profile from stream function is given by,

$$u = \frac{\partial \psi}{\partial y}, v = -\frac{\partial \psi}{\partial x}. \tag{3.17}$$

We know that $\psi = u_x \hat{i} + v_x \hat{j}$, and $v_x = 0$ for the flow problem, so we get the desired equation of the streamlines of the flow as

$$\psi = u_x = \frac{\partial u}{\partial x} = C_1 N\, SinhNy + C_2 CoshNy + \left(\left(\frac{\gamma}{N(1+\gamma)}\right)\frac{dp}{dx}\right)\left(SinhNy\right) - \left(\frac{G_m \gamma}{1+\gamma}\right)\left(\frac{1}{k^2 - N^2}\right)\frac{kCoshk(y-h_1)}{Sinhk(h_2-h_1)}. \tag{3.18}$$

4. Interpretation of Results

This section gives numerical simulations with the aid of graphs. The numerical simulations are performed using the computational software Mathematica.

4.1 Pressure Distribution

Figure 2 illustrates the behaviour of numerous embedding parameters on pressure gradient for a given wavelength versus x. The channel walls dp/dx are relatively small, thus helps the fluid in this region flow easily. The middle of the channel dp/dx is large, so relatively much pressure needed for the fluid to pass inside the region. Figure 2a depicts the variation in pressure gradient due to a change in Hartmann number M. Magnetic field parameter M raises the value of pressure gradient; fluid flow requires more pressure gradient to pass through the region. The effect of a fluid parameter γ can be seen in Figure 2b. A rise in fluid parameter γ decreases the pressure gradient.

Similarly, the impact of the phase difference can be seen in Figure 2c. In the narrow part of the channel, there is a decrease in pressure gradient when there is a rise in phase difference and a rise in pressure in the broader part of the channel when we decrease phase difference. Figure 2d and 2e Depict the magnitude of pressure gradient decreases by increasing the Schmidt number Sc and chemical reaction parameter R'.

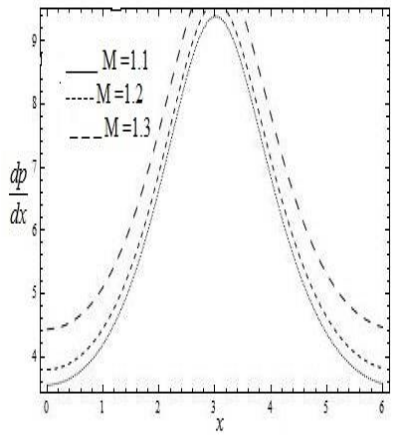

(a)

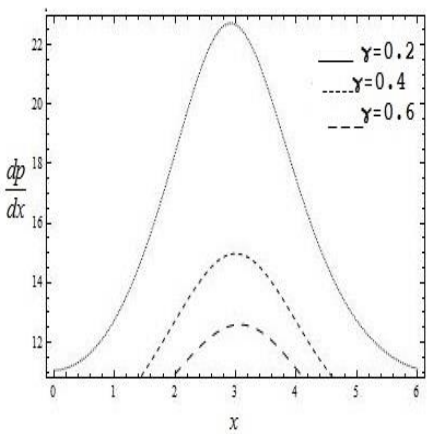

(b)

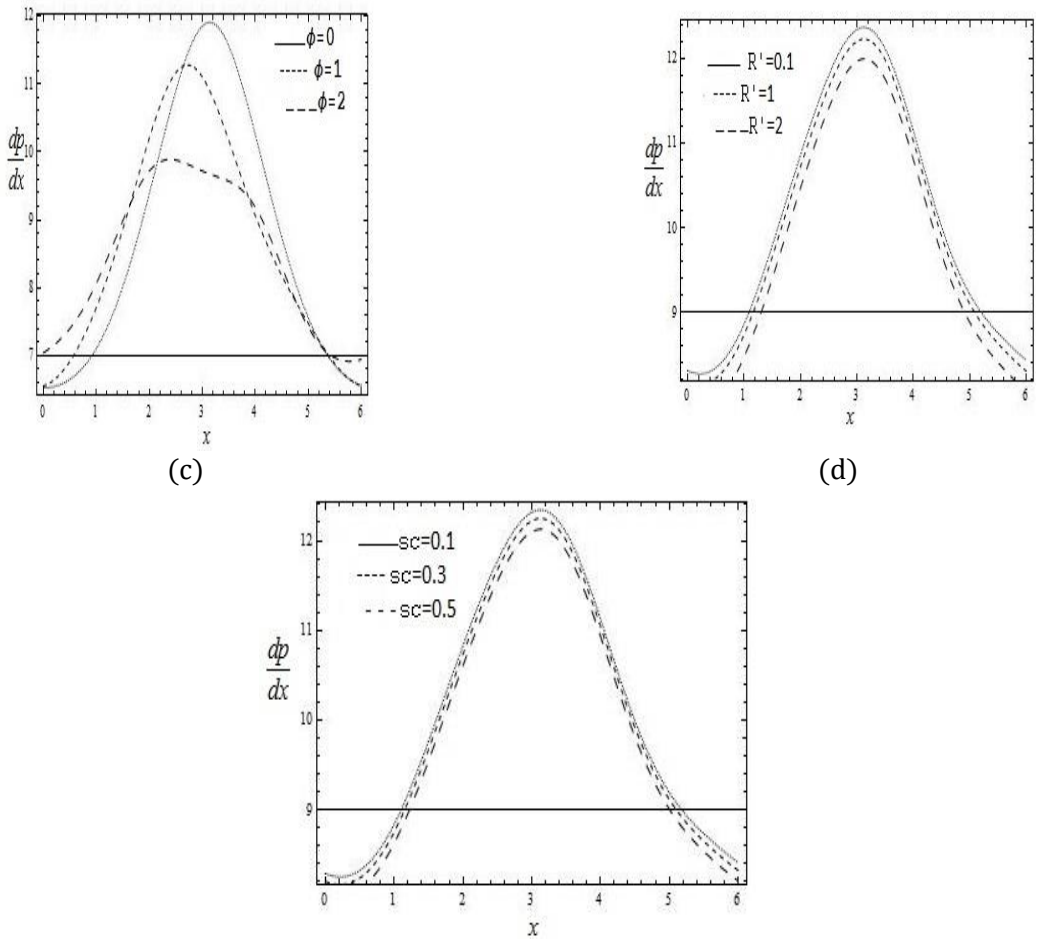

Figure 2. The figure represents variations of dp/dx versus x for $M, \gamma, \phi, R^{'}$ respectively.

In Figure 2a, when $a = 0.1, b = 0.5, \phi = 0.6, d = 1, Sc = 0.7, M, \gamma, \phi, R^{'} = 2, \gamma = 3$.

In Figure 2b when $a = 0.1, b = 0.5, \phi = 0.6, d = 1, Sc = 0.7, R^{'} = 2, M = 3$.

In Figure 2c when $a = 0.1, b = 0.5, d = 1, Sc = 0.7, R^{'} = 2, M = 3$.

In Figure 2d when $a = 0.1, b = 0.5, d = 1, Sc = 0.7, \phi = 0.6, \gamma = 3, M = 3$.

In Figure 2e when $b = 0.5, a = 0.1, d = 1,$.

4.2 Flow Rate Distribution

Figure 3 depicts the change in pressure rise ΔP versus flow rate Q for various parameters $\gamma, M, d, \phi, R^{'}, Sc$. Figure 3a Illustrates a non-linear relation between the pressure rise ΔP and flow rate Q. It is observed that higher the value of γ there is a drastic decrease in pressure rise, leading to a decline in the peristaltic pumping rate. Similar behaviour can be seen for the magnetic field M in Figure 3b below. Figure 3c Illustrates that pressure rise ΔP slowly decreases with an increase in d. But in Figure 3d, we can observe that rise in values of ϕ suddenly enhances the pressure rise. In Figure 3e and 3f, it is noted that higher the numbers of there is a linearly increase in pressure rise, leading to rise in the peristaltic pumping rate.

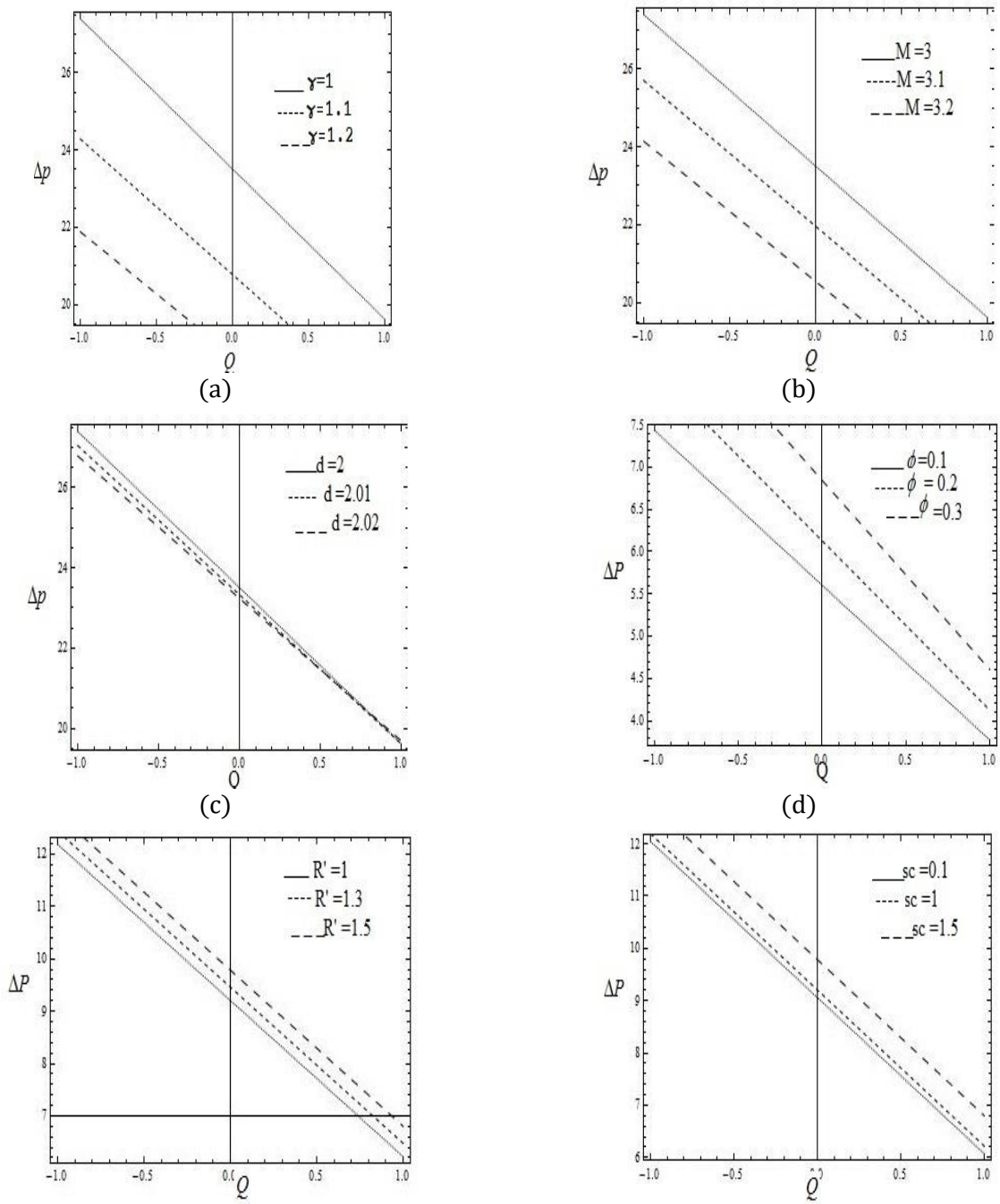

Figure 3. The figure represents variations in pressure rise ΔP versus Q for different values of $\gamma, M, d, \phi, R', Sc$ of respectively.

In Figure 3a when $a = 0.1, b = 0.5, d = 2, \phi = 0.5, Sc = 1.5, M = 3, R' = 2$.

In Figure 3b when $a = 0.1, b = 0.5, d = 2, \phi = 0.5, \gamma = 1, Sc = 1.5, R' = 2$.

In Figure 3c when $a = 0.1, b = 0.5, \phi = 0.5, \gamma = 1, Sc = 1.5, R' = 2, M = 3$.

In Figure 3d when $a = 0.1, b = 0.5, d = 2, \gamma = 2, Sc = 0.3, R' = 1, M = 2$.

In Figure 3e when $a = 0.1, b = 0.5, d = 2, \phi = 0.7, \gamma = 2, Sc = 1.5, M = 3$

In Figure 3f when $a = 0.1, b = 0.5, d = 2, \phi = 0.7, \gamma = 2, R' = 1.5, M = 3$

4.3 Concentration Profile

Figure 4 illustrates the concentration profile for numerous parameters a, b, d, ϕ, R', Sc, respectively. In Figure 4a, we can observe that enhance in Schmidt number Sc gradually minimizes the concentration profile. Figure 4b Shows the same behaviour as the reaction parameter slowly declines the concentration profile. In Figure 4c, we observed that the amplitude value a diminishes the concentration field. Similarly, in Figure 4d, we notice that the parameter b suddenly decreases the concentration field. Figure 4e Illustrates those higher parameter values d reduces the concentration profile. But in Figure 4f, we can see that higher phase difference values drastically enhance the concentration profile.

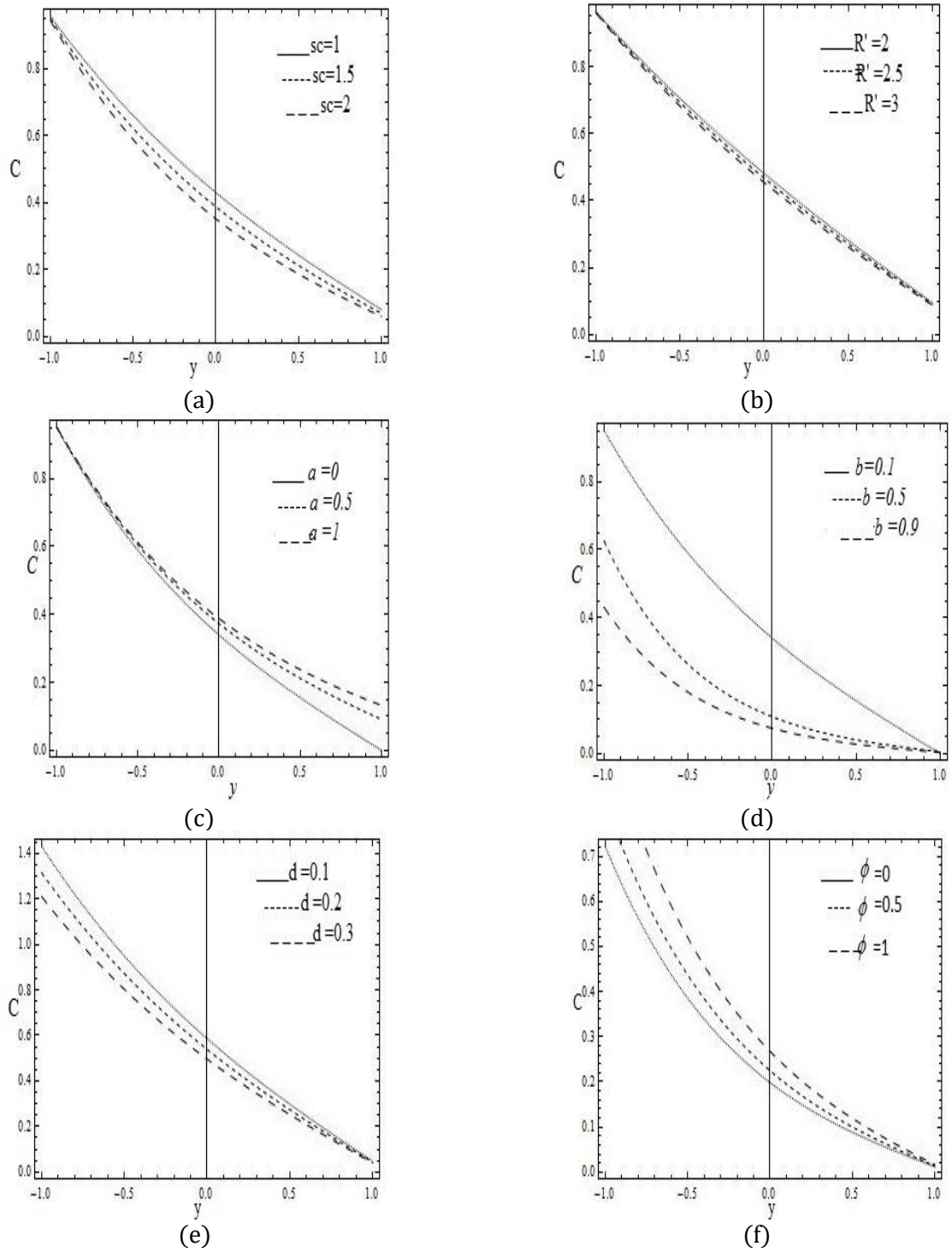

Figure 4. The figure represents variations of C versus y for Sc, R', a, b, d, ϕ respectively.

In Figure 4a when $a = 0.3, b = 0.1, d = 1, \phi = 0.4, R^{'} = 0.4$.

In Figure 4b when $a = 0.3, b = 0.1, d = 1, \phi = 0.4, Sc = 0.1$.

In Figure 4c when $b = 0.1, d = 1, \phi = 0.5, Sc = 1.5, R' = 0.5$.

In Figure 4d when $a = 0.1, d = 1, \phi = 0.5, Sc = 1.5, R^{'} = 2$.

In Figure 4e when $a = 0.1, b = 0.5, \phi = 0.3, Sc = 0.5, R^{'} = 1, \mathrm{x} = 0.1$

In Figure 4f when $a = 0.1, b = 0.3, \mathrm{d} = 1, Sc = 1.5, R^{'} = 1$

4.4 Trapping Phenomena

The streamlines are the imaginary lines in a fluid flow such that tangent at any position on a streamline will provide us with the velocity at that point. These lines will exhibit the direction in which a zero-rest mass fluid element will travel at any instant of time. The accumulation of bolus of the fluid in the closed streamlines inside a wave frame is called trapping. The nature of the streamlines against fluid parameter $\beta = 0.1, 0.5, 1.0, 5.0$, respectively, as shown in Figures 5. The fluid's viscosity relies on the parameter β, and it comes out to be highly viscous and turns thicker as we enhance the value of the Casson fluid parameter. Moreover, with the raising the values of the fluid parameter, the bolus will drastically shift to the middle of the channel, and the coupling streamlines sight below the wall.

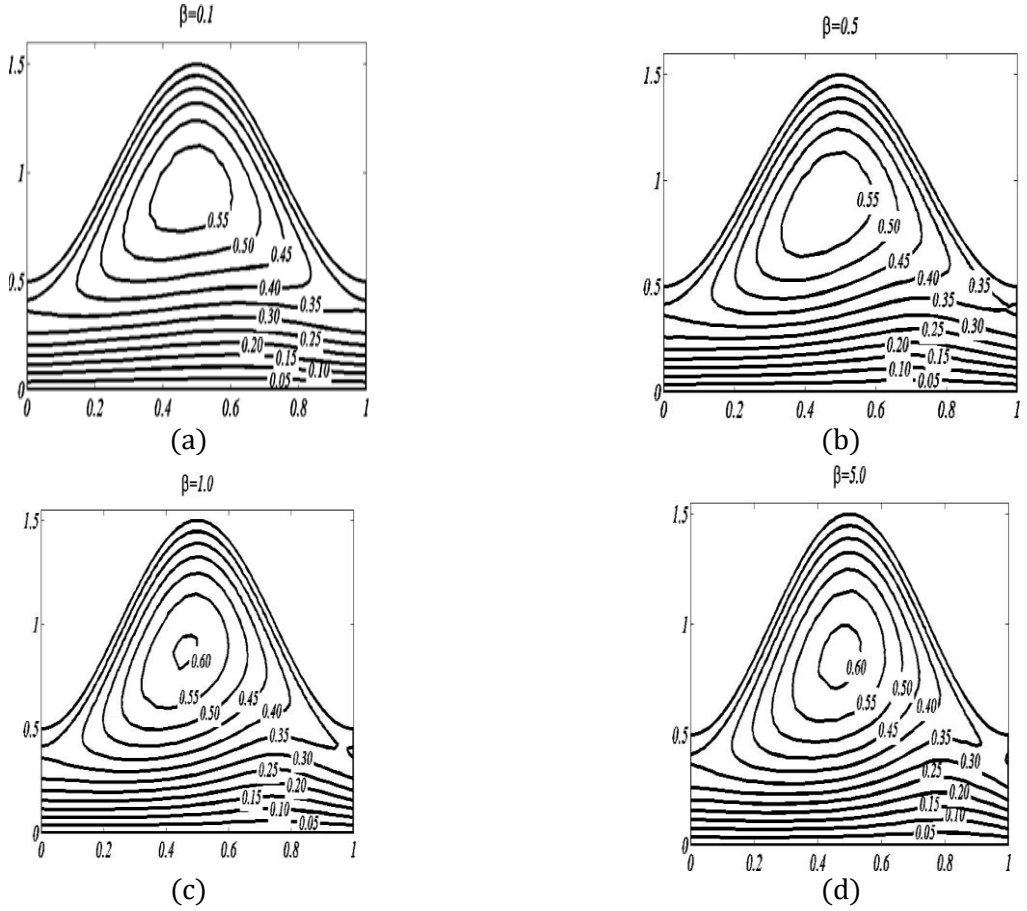

Figure 5. The figure represents streamlines against various values of β in wave frame with $Q = 1.3, a = 0.2, M = 2, \phi = 0.5.$

5. Conclusion

The mass transfer and MHD analysis on peristaltic motion of Casson fluid model embedded with porous medium and asymmetric geometry were considered. The influence of various pertinent governing flow parameters on the fluid model has been analysed with graphs. The concluding points of the present study are stated below.

1. At the centre of the channel, the amount of pressure gradient enhances when there is a magnetic field. But pressure gradient diminishes with an ascendance in parameters like $a = 0.1, b = 0.3, \mathrm{d} = 1, Sc = 1.5, R^{'} = 1.$

2. It is noted that pressure rise decreases with the increase in $\gamma, M, R^{'}, Sc$ and d . However, it increases with an increase in phase difference.

3. The concentration profile reduces when there is a rise in parameters like $a, b, d, R^{'}$ and Sc . However, it increases when we increase the value ϕ .

4. It is equal in value to observe that increase in the Schmidt parameter Sc and chemical reaction term $R^{'}$ decreases the concentration profile.

5. We observe a reduction in both pressure rise and pressure gradient when we enhance values of Schmidt number Sc and reaction parameter $R^{'}$.

Author Contributions

All authors contributed equally to this work. They all read and approved the final version of the manuscript.

Conflicts of Interest

The authors declare no conflict of interest.

6. References

[1] W. M. Bayliss, E. H. Starling, *Physiology of Peristalsis*, Journal of Physiology (London), 24, (1899) 99–143.

[2] T. W. Latham, *Fluid motion in a peristaltic pump*, Master's Thesis, Massachusetts Institute of Technology (1986), Cambridge, USA.

[3] K. K. Raju, R. Devanathan, *Peristaltic motion of a non-Newtonian fluid*", *Rheologica Acta*, 11, (1972) 170–179.

[4] N. S. Akbar, *Influence of magnetic field on peristaltic flow of a Casson fluid in an asymmetric channel*, application in crude oil refinement. Journal of Magnetism and Magnetic Materials, 378, (2015) 463–468.

[5] K. Ramesh, M. Devakar, *Some analytical solutions for flows of Casson fluid with slip boundary conditions*, Ain Shams Engineering Journal, 6(3), (2015) 967–975.

[6] M. Rashidi, M.Yang, Z. Bhatti, M. M Bhatti, M. A. Abbas, *Heat and mass transfer analysis on MHD blood flow of Casson fluid model due to peristaltic wave*, Thermal Science, 22(6 (A)), (2018) 2439–2448.

[7] V. P. Rathod, L. Devindrappa, *Peristaltic transport in an inclined asymmetric channel with heat and mass transfer by Adomian decomposition method*, Advances in Applied Science Research, 7, (2016) 83–100.

[8] N. Iftikhar, A. Rehman, H. Sadaf, M. N. Khan, *Impact of wall properties on the peristaltic flow of Cu-water nanofluid in a non-uniform inclined tube*, International Journal of Heat and Mass Transfer, 125, (2018) 772–779.

[9] B. B. Divya, G. Manjunatha,C. Rajashekhar, H. Vaidya, K. V. Prasad, *The hemodynamics of variable liquid properties on the MHD peristaltic mechanism of Jeffrey fluid with heat and mass transfer*, Alexandria Engineering Journal, 59(2), (2020) 693–706.

[10] K. Ahmed, R. Nazar, *Magnetohydrodynamic three-dimensional flow and heat transfer over a stretching surface in a visco-elastic fluid*, Journal of Science and Technology, 3(1), (2011) 33–46.

[11] S. Nadeem, R. U. Haq, C. Lee, *MHD flow of a Casson fluid over an exponentially shrinking sheet*, Scientia Iranica, 19, (2012) 1550–1553.

[12] Z. Asghar, N. Ali, R. Ahmed, M. Waqas, W. A. Khan, *A mathematical framework for peristaltic flow analysis of non-Newtonian Sisko fluid in an undulating porous curved channel with heat and mass transfer effects*, Computer Methods and Programs in Biomedicine, 182, (2019) 105040.

[13] S. Nadeem and S. Akram, *Slip effects on the peristaltic flow of Jeffrey fluid in an asymmetric channel under the effect of induced magnetic field*, International Journal for Numerical Methods in fluids, 63, (2010) 374–394.

[14] [14] S. Hina, *MHD peristaltic transport of Eyring-Powell fluid with heat/mass transfer, wall properties and slip conditions*, Journal of Magnetism and Magnetic Materials, 404, (2016) 148–158.

[15] M. Gnaneswara Reddy, *Heat and Mass transfer on Magnetohydrodynamic peristaltic flow in a porous medium with partial slip*, Alexandria Engineering Journal, 55, (2016) 1225–1234.

[16] S. Akram, S. Nadeem, *Influence of induced magnetic field and heat transfer on the peristaltic motion of a Jeffrey fluid in an asymmetric channel: closed-form solution*, Journal of Magnetism and Magnetic Materials, 328, (2013) 11–20.

[17] M. Gnaneswara Reddy, K. Venugopal Reddy, D. O. Makinde, *Heat transfer on MHD peristaltic rotating flow of a Jeffrey fluid in an asymmetric channel*, International Journal of Applied and Computational Mathematics, 3, (2016) 3201–3227.

[18] T. Sarpakaya, *Flow of non-Newtonian fluids in a magnetic field,* American Institute of Chemical Engineers Journal, 7, (1961) 324–328.

[19] T. Hayat, A. Saleem, A. Tanveer, F. Alsaadi, *Numerical study for MHD peristaltic flow of Williamson nanofluid in an endoscope with partial slip and wall properties*, International Journal of Heat and Mass Transfer, 114, (2017) 1181–1187.

[20] C. Vasudev, U. Rajeswara Rao, M. V. Subba Reddy, G. Prabhakar Rao, *Influence of Magnetic field and Heat transfer on Peristaltic flow of Jeffrey fluid through a porous medium in an asymmetric channel*, ARPN Journal of Engineering and Applied Sciences, 5, (2010) 87–103.

[21] V. P. Rathod, Laxmi Devindrappa, *Effects of heat transfer on the peristaltic MHD flow of a Bingham fluid through a porous medium in a channel*, International Journal of biomathematics, 7, (2014) 1450060–1450080.

[22] V. P. Rathod, M. M. Channakote, *Slip effects and heat transfer on MHD peristaltic flow of Jeffrey fluid in an inclined channel*, Journal of Chemical, Biological and Physical Sciences, 2, (2012) 1987–1997.

[23] A. Zeeshan, M. M. Bhatti, T. Muhammad, L. Zhang, *Magnetized peristaltic particle-fluid propulsion with Hall and ion slip effects through a permeable channel,* Physica A: Statistical Mechanics and its Applications, 550, (2019) 123999.

[24] R. Muthuraj, K. Nirmala, S. Srinivas, *Influence of chemical reaction and wall properties on MHD peristaltic transport of a dusty fluid with heat and mass transfer*, Alexandria Engineering Journal, 55, (2016) 597–611.

[25] T. Hayat, S. Hina, A. A. Hendi, S. Asghar, *Influence of compliant walls on peristaltic motion with heat/mass transfer and chemical reaction*, International Journal of Heat and Mass Transfer, 55, (2012) 3386–3394.

[26] T. Hayat, H.Yasmin, M. Al-Yami, *Soret and Dufour effects in peristaltic transport of physiological fluids with chemical reaction: A mathematical Analysis*, Computers and Fluids, 70, (2014) 242–253.

[27] T. Hayat, H. Zahir, A. Tanveer, A. Alsaedi, *Influence of Hall current and chemical reaction in mixed convective peristaltic flow of Prandlt fluid*, Journal of Magnetism and Magnetic materials,407, (2016) 321–327.

[28] M. G. Reddy, K. V. Reddy, *Influence of Joule heating on MHD peristaltic flow of a nanofluid with compliant walls*, Procedia Engineering, 127, (2015) 1002–1009.

[29] K. V. Reddy, O. D. Makinde, M. G. Reddy, *Thermal analysis of MHD electro-osmotic peristaltic pumping of Casson fluid through a rotating asymmetric micro-channel*, Indian Journal of Physics, 92(11), (2018) 1439–1448.

[30] M. G. Reddy, B. C. Prasannakumara, O. D. Makinde, *Cross diffusion impacts on hydromagnetic radiative peristaltic Carreau-Casson nanofluids flow in an irregular channel*, Defect and Diffusion Forum, 377, (2017) 62–83.

[31] O. D. Makinde, M. Gnaneswara Reddy, K. Venugopal Reddy, *Effects of Thermal Radiation on MHD Peristaltic Motion of Walters-B Fluid with Heat Source and Slip Conditions*, Journal of Applied Fluid Mechanics, 10(4), (2017) 1105–1112.

[32] M. Gnaneswara Reddy, K. Venugopal Reddy, O. D. Makinde, *Hydromagnetic peristaltic motion of a reacting and radiating couple stress fluid in an inclined asymmetric channel filled with a porous medium,* Alexandria Engineering Journal, 55(2), (2016) 1841–1853.